

# 0°–360° bistable nematic liquid crystal display with large $d\Delta n$ and high contrast

Z. L. Xie,<sup>a)</sup> C. Y. Zheng, S. Y. Xu, and H. J. Gao

*Department of Chemistry, Beijing Tsinghua Engineering Research Center for Liquid Crystal Technology, Tsinghua University, Beijing 100084, People's Republic of China*

H. S. Kwok

*Department of Electronic and Electrical Engineering, Center for Display Research, Hong Kong University of Science and Technology, Clear Water Bay, Hong Kong*

(Received 31 August 1999; accepted for publication 16 March 2000)

A new mode of 0°–360° bistable twisted nematic (BTN) liquid crystal display is developed by using a parameter space method. This new mode possesses a large  $d\Delta n$  value that provides a possibility of using a 4.8–7  $\mu\text{m}$  cell gap and a 6.5 V operating voltage for the new 0°–360° BTN cells. The high-contrast ratios above 80 within  $-80^\circ$ – $80^\circ$  viewing-angle ranges are obtained experimentally in a horizontal direction, and the highest contrast ratio achieved is up to 250. In the contrast ratio, the experiment's results concur with the simulation results. © 2000 American Institute of Physics. [S0021-8979(00)06512-9]

## I. INTRODUCTION

A bistable twisted nematic (BTN) liquid crystal display (LCD) that can be switched between two metastable twisted states was discovered by Berreman and Heffner<sup>1</sup> in 1981. Recently, Tanaka *et al.*<sup>2</sup> successfully made use of this bistability to develop a 0°–360° bistable LCD with a black–white VGA image. This display can be passive-matrix driven, and it has the characteristics of a wide-viewing angle and a good contrast ratio. Therefore, there have been many studies on improving this transmissive BTN LCD mode.<sup>3–14</sup> So far, most of the reports<sup>3–11</sup> are concentrated in this 0°–360° BTN mode, namely, the ‘‘Tanaka’s mode.’’

However, there is a critical problem in the Tanaka’s mode.<sup>2</sup> The problem is that its cell gap must be selected at about 2  $\mu\text{m}$  because of its small  $d\Delta n$  value ( $\approx \lambda/2$ ). For such a narrow gap, a short circuit will be produced very easily when an operating voltage (normally above 20 V) is applied to the BTN cell. Moreover, an ultraclean environment will be required in manufacturing this BTN LCD to avoid any small particle ( $\geq 2 \mu\text{m}$ ) to be sandwiched in the small gap. Hence a special technique should be adopted to eliminate such short circuits, and some more expensive instruments should be equipped to keep the environment clean. Otherwise, much waste will occur in industrial fabrication.

In order to overcome the problem mentioned above, in this article we develop a new 0°–360° BTN mode by using a parameter space method.<sup>15</sup> The new mode possesses larger  $d\Delta n$  and higher contrast ratio than Tanaka’s mode, and it can provide the possibility of using a large cell gap and low operating voltage for 0°–360° BTN LCD in practical fabrication.

## II. OPTICAL OPTIMIZATION OF 0°–360° BTN

For the case of a transmissive BTN, the static parameter space is ideal in analyzing its optical properties since both bistable twist states operate at zero voltage. Figure 1 shows the structure schematic drawing of a transmissive BTN LCD. Clearly, a liquid crystal cell is placed between two polarizers, and the input and output polarizer axes are at an angle of  $\alpha$  and  $\gamma$ , respectively to the input director of the liquid crystal cell. The transmission of this optical arrangement is given by

$$T = \left| (\cos \gamma \sin \gamma) \cdot M \cdot \begin{bmatrix} \cos \alpha \\ \sin \alpha \end{bmatrix} \right|^2. \quad (1)$$

For the case of  $\gamma = \alpha + 90^\circ$ , Eq. (1) leads to the following expression:

$$T = \left| (-\sin \alpha \cos \alpha) \cdot M \cdot \begin{bmatrix} \cos \alpha \\ \sin \alpha \end{bmatrix} \right|^2. \quad (2)$$

The  $M$  is the Jones matrix for the LC cell, and it is a function of a LC-twist angle  $\phi$ , a thickness-birefringence product  $d\Delta n$ , an input-light wavelength  $\lambda$ , and a LC pretilt angle  $\theta$ . In this article, we fix  $\lambda$  at 550 nm,  $\theta$  at 0°. Therefore for 0°–360° BTN, the transmission  $T$  of its 0° or 360° twist states is a unique function of  $d\Delta n$  and  $\alpha$ . So the contrast ratio (CR), which is defined as  $\text{CR} = T(0)/T(360)$  or  $T(360)/T(0)$ , can be plotted as a unique function of  $d\Delta n$  and  $\alpha$  in a two-dimensional contour map.

Figure 2 shows the dependence of the contrast ratio on  $\alpha$  and  $d\Delta n$  for a 0°–360° BTNLC cell with cross-polarizer geometry. Each contour line in Fig. 2 represents an increase of 37 in the contrast ratio. Clearly, two large regions, labeled with characters *A* and *B*, respectively, possess excellent contrast ratio. Region *A* has a small  $d\Delta n$  value and is located near the point of  $\alpha = 45^\circ$ ,  $d\Delta n = 0.16 \mu\text{m}$  in the  $(\alpha, d\Delta n)$  parameter space. Its contrast ratio is over 112 and is not sensitive to the change in  $\alpha$ . In fact, region *A* includes the

<sup>a)</sup>Author to whom correspondence should be addressed; electronic mail: chxie@public.east.cn.net

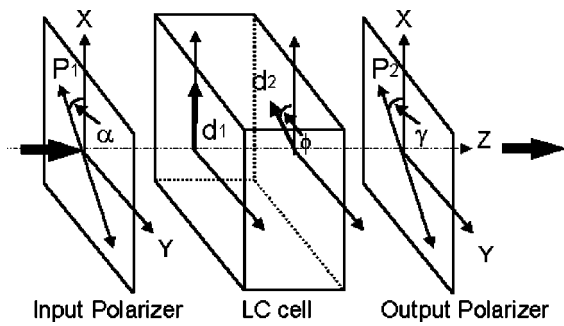


FIG. 1. The structure schematic drawing of a transmissive BTN LCD.

operating point proposed by Tanaka, as well as the operating points of the other previous reports of  $0^\circ\text{--}360^\circ$  BTN. In addition, region *B* possesses a large  $d\Delta n$  value and is located near the point of  $\alpha=0^\circ$ ,  $d\Delta n=0.78\ \mu\text{m}$ . The contrast ratio in region *B* is more than 149 and is not sensitive to the change in  $d\Delta n$ . Hence we can select a new operating point in region *B* to obtain a large  $d\Delta n$  value and a high contrast ratio for a  $0^\circ\text{--}360^\circ$  BTN LC cell.

### III. RESULTS AND DISCUSSION

To investigate the new  $0^\circ\text{--}360^\circ$  BTN mode, we made three LC cells with antiparallel-rubbing directions on two alignment layers of the cells. A commercial polyamide SN-7321 (Merck) was used as an alignment layer with an  $11^\circ$  pretilt angle. The  $d/P_0$  values of the cells were controlled near 0.6 by a chiral additive S-811, where  $d$  is a cell gap and  $P_0$  is a LC inherent pitch. These cells with different gaps (7, 5, and  $4.8\ \mu\text{m}$ ) were filled with different commercial LC materials, respectively, thus their  $d\Delta n$  values are 0.73, 0.74, and 0.76, respectively, and they are included in region *B*. The detailed parameters of the three cells are listed in Table I. The  $0^\circ$  and  $360^\circ$  twist states of the new mode can be clearly distinguished by the birefringence effect in the system including the LC cell and polarizers, since the input-polarizer direction was put parallel to the LC input director as well as perpendicular to the output polarizer.

Figure 3 shows a driving wave form to switch the three cells mentioned above consists of a reset pulse to switch LC molecules to a near-homeotropic state, followed by a selection pulse to select either of two metastable states. The reset

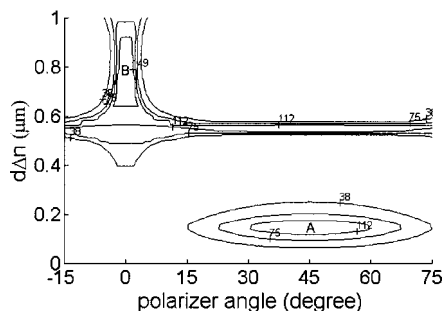


FIG. 2. Parameter space showing contours of contrast ratio vs input polarizer  $\alpha$  and  $d\Delta n$  for  $0^\circ\text{--}360^\circ$  BTN cell with cross polarizer geometry (input and output polarizer directors are perpendicular).

TABLE I. Various parameter values of three  $0^\circ\text{--}360^\circ$  BTN cells.

	Cell 1	Cell 2	Cell 3
LC	7500/000	5700/100	6204/000
$\Delta n$	0.1039	0.1581	0.1478
$\Delta\epsilon$	10.2	25.8	35.5
$d(\mu\text{m})$	7.0	4.8	5.0
$d\Delta n(\mu\text{m})$	0.73	0.76	0.74

time and reset amplitude are represented by  $Tr$  and  $Vr$ , respectively, and the selection time and the selection amplitude are represented by  $Ts$  and  $Vs$ , respectively. Being somewhat complex, the driving wave form is the most suitable and practical for switching the BTN cell, because it can be easily divided into common-scanning signal and segment-data signal to facilitate passive-matrix addressing. Actually Tanaka *et al.* have successfully applied this wave form to drive their  $0^\circ\text{--}360^\circ$  BTN LCD. We believe that this wave form is also suitable for driving the new  $0^\circ\text{--}360^\circ$  BTN mode.

Figure 4 shows the time-dependent transmission curve and the time-dependent voltage pulse for the three cells switched by the wave form in Fig. 3. In this measurement, the  $Tr$ ,  $Vr$ , and  $Ts$  are fixed at 12 ms, 14 V, and 4 ms, and the  $Vs$  alternates between 0 and 5 V. Clearly, for the three cells, their  $0^\circ$  twist states, which correspond to low transmission can be obtained by a 5 V selection pulse, while their  $360^\circ$  twist states, which correspond to high transmission, can be obtained by a 0 V selection pulse. Moreover, their contrast ratios measured between  $0^\circ$  and  $360^\circ$  states are over 100:1 in a normal direction. Both  $0^\circ$  and  $360^\circ$  states can remain for several seconds after the electric field is removed, and if they show true black and buff, respectively, then they will relax to a stable  $180^\circ$  twist state. Indeed the  $0^\circ$  and  $360^\circ$  twist states are metastable, and they can be obtained for the three cells by using the switching wave form in Fig. 3.

Besides various cell gaps, several different LC materials with different  $\Delta\epsilon$  values were used for the three cells. When  $Tr$ ,  $Ts$ , and  $Vs$  are invariable, the change of a  $\Delta\epsilon$  value has a great influence on  $Vr$ . Figure 5 shows the dependence of the minimum  $Vr$  on the  $\Delta\epsilon$  of LC material for the new mode cells. Obviously, the minimum  $Vr$  is decreased approximately linearly as the  $\Delta\epsilon$  is increased. For example, if the  $Tr$ ,  $Ts$ , and  $Vs$  are fixed at 45 ms,  $Tr/3$ , and  $Vr/4$ , the minimum  $Vr$  can be reduced from 12 to 6.5 V as the  $\Delta\epsilon$  is increased from 10.2 to 35.5. On the other hand, the  $Tr$  will evidently

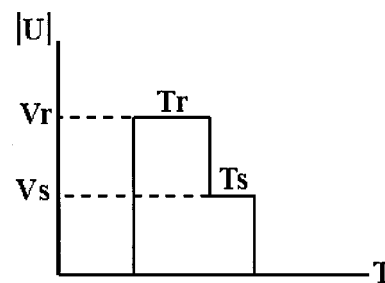


FIG. 3. Switching wave form for driving  $0^\circ\text{--}360^\circ$  BTN cell.

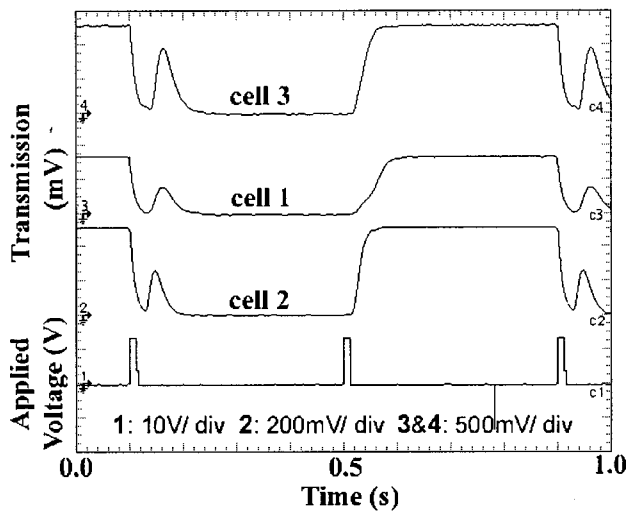


FIG. 4. Transmission of three LC cells (upper three) and applied voltage pulse (bottom) as a function of time. The  $0^\circ$  twist state has low transmission and the  $360^\circ$  twist state has high transmission.

effect on the minimum  $V_r$  as shown in Fig. 5. When the  $\Delta\epsilon$ ,  $T_s$ , and  $V_s$  are fixed at 35.5,  $T_r/3$ , and  $V_r/4$ , the minimum  $V_r$  can be reduced from 11 to 6.5 V as the  $T_r$  is increased from 5.6 to 45 ms. Although both a high  $\Delta\epsilon$  and a long  $T_r$  can decrease  $V_r$  for the new mode, it is better to choose a high  $\Delta\epsilon$  value to do that, since a long  $T_r$  will lead to slow video frequency for display.

In addition, a long  $T_r$  also has an influence on  $V_s$  for the new mode, and the experimental results of such an influence are shown in Fig. 6. In our experiments, the  $V_r$  and  $T_s$  are fixed at 20 V and 10 ms. When the  $T_r=30$  ms, the  $0^\circ$  twist state corresponding to low transmittance is selected within a finite amplitude range between 4 and 8 V (Fig. 6). Beyond this range, the  $360^\circ$  twist state is obtained in ranges of below 2 V and above 10 V. Moreover, when  $T_r$  is increased to 60 ms, the selection range of the  $0^\circ$  twist state becomes very narrow and is located near 6 V, and it is too narrow to make passive matrix addressing for the new mode. So these results seem to indicate that a long  $T_r$  is a disadvantage of the new mode. However, no remarkable change of the selection

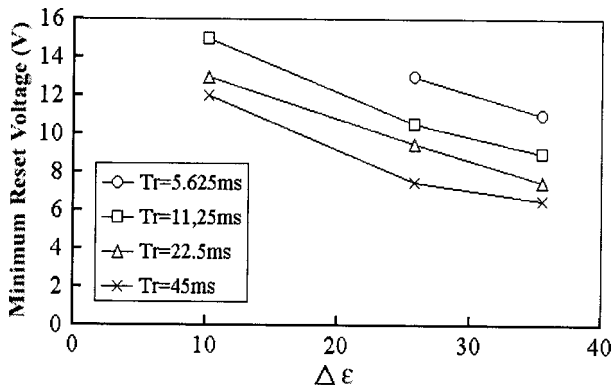


FIG. 5. Relationship between the minimum  $V_r$  and the  $\Delta\epsilon$  of LC material, where  $T_r=45$  ms,  $V_s=V_r/4$  and  $T_s=T_r/3$ . The wave form in Fig. 3 is used to switch the new mode cell.

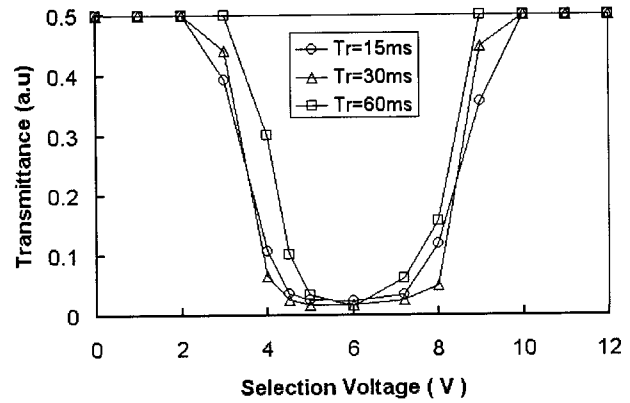


FIG. 6. Relationship between the reset time  $T_r$  and selection voltage  $V_s$ , where  $V_r=20$  V and  $T_s=10$  ms. The wave form in Fig. 3 is used.

ranges is found when the  $T_r$  is decreased from 30 to 15 ms. This probably means that a short  $T_r$  hardly influences  $V_s$  in some cases.

As has been known from Fig. 2, the contrast ratio over 149 in a normal direction can be obtained in region B. Furthermore, the relationship between contrast ratio and viewing angle was investigated for the new mode both in a horizontal and vertical direction. Figure 7 shows the experimental results and simulation results in a horizontal viewing direction. Surprisingly, for the experimental curve (dashed line), the contrast ratios above 160 can be obtained within the  $-70^\circ$ – $70^\circ$  viewing angles, and they can also be obtained above 80 between the  $-80^\circ$  and  $80^\circ$  viewing angles. Importantly the highest contrast ratio of 250 can be obtained at a  $-50^\circ$  viewing angle. It is the first time to achieve such a high contrast ratio in so wide a viewing-angle range for BTN LCD. In addition, both experimental and simulation curves (real line) shows an asymmetry, and their contrast peak values on the left are higher than those on the right since the pretilt angle of liquid crystal on the alignment layer is  $11^\circ$  instead of  $0^\circ$ . Clearly, the simulation results agree with the experimental

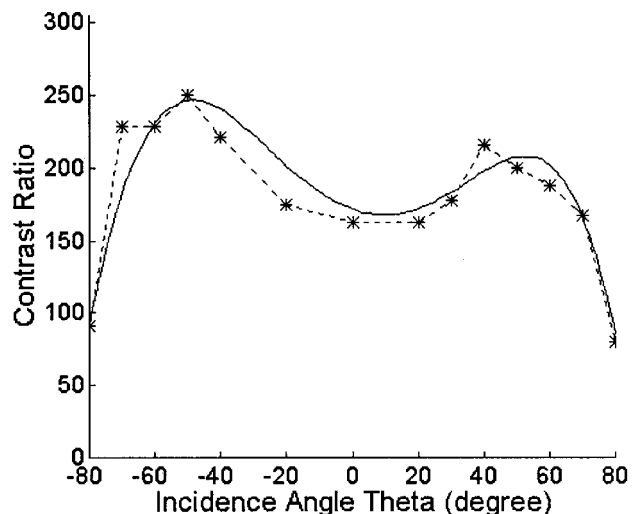


FIG. 7. Relationship between contrast ratio and viewing angle in horizontal viewing direction. The experimental results and simulation results are represented by dashed line and real line, respectively.

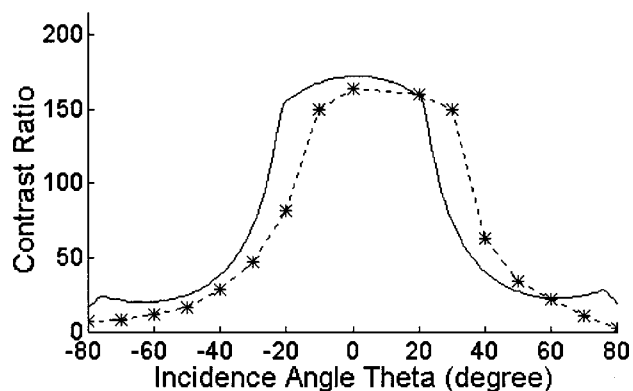


FIG. 8. Relationship between contrast ratio and viewing angle in vertical viewing direction. The experimental results and simulation results are represented by dashed line and real line, respectively.

results very well. That means our simulation method is accurate and effectual for the BTN cell.

Figure 8 shows the experimental and simulation results in a vertical direction. Obviously, both the experimental curve (dashed line) and the simulation curve (real line) have the same shape, but the experimental curve locates slightly to the right of the simulation one. In Fig. 8, the contrast ratios can be obtained above 80 between the  $-20^\circ$  and  $40^\circ$  viewing angles, and they can be obtained above 30 from  $-40^\circ$  to  $55^\circ$  in the viewing angle. Compared with that in Fig. 7, the range of high contrast ratio becomes narrower in Fig. 8. This indicates that the contrast ratio in a horizontal viewing direction is better than that in a vertical viewing direction for the new mode.

#### IV. CONCLUSION

In summary, in order to overcome the drawback of a small cell gap in Tanaka's mode, a new mode of  $0^\circ$ – $360^\circ$  BTN LCD is developed by using a parameter space method. The new mode has a larger  $d\Delta n$  and a higher contrast ratio than those of the Tanaka's mode. The large  $d\Delta n$  value has at

least two advantages. One is that a large cell gap (from  $4.8$  to  $7 \mu\text{m}$ ) can be adopted in practical fabrication so that the new  $0^\circ$ – $360^\circ$  BTN LCD can be manufactured with good yield. Another one is that large  $\Delta\epsilon$  liquid crystal material can be used to reduce the operating voltage to  $6.5$  V. This means that we can use inexpensive integrated circuits and save power consumption. Besides, the high contrast ratios above 80 within the  $-80^\circ$ – $80^\circ$  viewing angles in a horizontal direction are obtained experimentally for the new mode, and the highest contrast ratio achieved is up to 250. This will much improve the display quality of  $0^\circ$ – $360^\circ$  BTN LCD.

Compared with Tanaka's mode, the new mode also has some shortcoming itself such as low light efficiency of the bright state and nonblack–white display. Nevertheless, its brightness can be enhanced by using a powerful backlight, and its black–white display can be carried out by adding a suitable retardation film to the LC cell. This work will be done in the future.

- <sup>1</sup>D. W. Berreman and W. R. Heffner, *J. Appl. Phys.* **52**, 3032 (1981).
- <sup>2</sup>T. Tanaka, Y. Sato, A. Inoue, Y. Momose, H. Notuma, and S. Iino, *Proceedings Asia Display*, 1995, p. 259.
- <sup>3</sup>I. Dozov, M. Nobili, and G. Durand, *Appl. Phys. Lett.* **70**, 1197 (1997).
- <sup>4</sup>T. Z. Qian, Z. L. Xie, H. S. Kwok, and P. Sheng, *Appl. Phys. Lett.* **71**, 596 (1997).
- <sup>5</sup>C. D. Hoke, J. Li, J. R. Kelly, and P. J. Bos, *SID Symp. Dig.* **28**, 29 (1997).
- <sup>6</sup>J. C. Kim, G.-J. Choi, Y.-S. Kim, K. H. Kang, T.-H. Yoon, and K. G. Nam, *SID Symp. Dig.* **28**, 33 (1997).
- <sup>7</sup>H. S. Kwok, Z. L. Xie, T. Z. Qian, and P. Sheng, *Proc. SPIE* **3143**, 22 (1997).
- <sup>8</sup>H. S. Kwok, T. Z. Qian, Z. L. Xie, and P. Sheng, *Proceedings of the 17th IDRC Conference*, 1997, p. 89.
- <sup>9</sup>C. D. Hoke and P. J. Bos, *Proceedings of the 17th IDRC Conference*, 1997, p. 85.
- <sup>10</sup>G.-D. Lee, H.-S. Kim, T.-H. Yoon, J. C. Kim, and E.-S. Lee, *SID Symp. Dig.* **29**, 842 (1998).
- <sup>11</sup>H. Bock, *Appl. Phys. Lett.* **73**, 2905 (1998).
- <sup>12</sup>Z. L. Xie and H. S. Kwok, *Proceedings of the 4th IDW Conference*, 1997, p. 265.
- <sup>13</sup>Z. L. Xie and H. S. Kwok, *Jpn. J. Appl. Phys., Part 2* **37**, 2572 (1998).
- <sup>14</sup>Z. L. Xie, H. J. Gao, and H. S. Kwok, *SID Symp. Dig.* **29**, 846 (1998).
- <sup>15</sup>H. S. Kwok, *J. Appl. Phys.* **80**, 3687 (1996).